

Unfolding of phases and multicritical points in the Classical Anisotropic van Hemmen Spin Glass Model with Random Field

S. G. Magalhaes, I. C. Berger, R. Erichsen Jr.

Instituto de Física, Universidade Federal do Rio Grande do Sul, Porto Alegre, RS, Brazil

Abstract

We study magnetic properties of the 3-state spin ($S_i = 0$ and ± 1) spin glass (SG) van Hemmen model with ferromagnetic interaction J_0 under a random field (RF). The RF follows a bimodal distribution. The combined effect of the crystal field D and the special type of on-site random interaction of the van Hemmen model engenders the unfolding of the SG phases for strong enough RF, i. e., instead of one SG phase, we found two SG phases. Moreover, as J_0 is finite, there is also the unfolding of the mixed phase (with the SG order parameter and the spontaneous magnetization simultaneously finite) in four distinct phases. The emergence of these new phases separated by first and second order line transitions produces a multiplication of triple and multicritical points.

1. Introduction

Disorder effects in magnetic systems with localized spins considering random interaction, frustration and random fields are permanent sources of challenging issues. The simultaneous combination of these complex examples of disorder does exist in real systems. It can be found in $\text{Fe}_x\text{Zn}_{1-x}\text{F}_2$ and $\text{Fe}_x\text{Mg}_{1-x}\text{Cl}_2$ compounds [1]. More recently, spin glass and RF have been also suggested to exist in the diluted Ising-like dipolar ferromagnetic compound $\text{LiHo}_x\text{Y}_{1-x}\text{F}_4$ [2]. The existence of real systems with the combined presence of a spin glass (SG) phase and random field (RF) makes its description a quite relevant problem in the disordered magnetism with localized spins (see, for instance, Ref. [3]).

Such description has several obstacles. One of them concerns the use of replica method. In particular, the dispute about the existence of a replica symmetry breaking (RSB) in a Ising SG model as predicted by Parisi [4]. The crucial validation of this scenario would be the existence of the de Almeida-Thouless line [5]. This existence is still currently disputed by simulational techniques or even experimentally [6]. In addition, for 3-state disordered spins models, the

Email address: sgmagal@gmail.com (S. G. Magalhaes)

replica method presents others difficulties. These models are known by displaying tricritical points and, therefore, a first order line transition whose location is a complicated task within the replica method. For example, it is known that in the Gathak-Sherrington model at mean field level [7], the proper location of the first order line transition is far from obvious since the stability requirements do not provide proper guidance to select correctly the SG solution [8]. Indeed, the presence of a RF complicates the situation since the first order phase transition line is much affected by the RF [9, 10]. Another aspect that should be remarked is that the RF field induces the replica symmetric SG order parameter which becomes finite at any temperature. As a consequence, it is strictly necessary to find RSB SG solutions of the order parameters [11] which makes even more complicated the location of the first order line transition. That situation enforces the necessity to work with disordered spin models in the presence of RF which avoids the replica method.

We present in this work an analysis of the combined effect of random couplings and random fields in the 3-state spin ($S_i = 0$ and ± 1) van Hemmen model with a crystal field D , the so called anisotropic van Hemmen spin glass (AvHSG) model [12, 13]. This on site-disorder model was introduced as an exactly solvable model suitable to describe metallic SG without the use of the replica method. It has both fundamental ingredients for the SG phase, i. e., disorder and frustration. Although its infinite-range version does not present a complex free energy landscape with a large number of local minima [14], the van Hemmen model can account for several static properties of real SG systems. Another important aspect is that this model displays naturally mixed phases if a ferromagnetic interaction is also present. In this mixed phase the SG order parameter and the spontaneous magnetization are simultaneously finite. Its existence is deeply related to the special type of on-site random interaction of the van Hemmen model which are given as a product of local random variables [12, 13]. In the AvHSG model the number of sites with spins magnetically actives can no longer coincides with the number of site lattices N .

The combined effects of D and the uniform field h are well illustrated in a previous study of the AvHGS model performed by de Almeida and Moreira [15]. At $T = 0$, for small D and h , these authors found the usual spin glass phase with spin glass order parameter $q = 1/2$ and magnetization $m = 0$, as expected. Interestingly, for large h and D frustration is still favored. As consequence, there is the emergence of a new special type of mixed phase with $m = 1/2$ (induced by h) and SG order parameter $q = 1/4$. Moreover, at $T = 0$, the phase transition lines between paramagnetism (PM), SG and this mixed phase are all first order. At finite temperature, the phase transition lines are first and second order. As consequence, there are ordered critical and tricritical points.

The scenario described previously arises the question which are the consequences if the uniform field is replaced by a RF? While for small RF and D , one can expect the presence of the usual SG phase (as found in the case with uniform field), it is far from obvious what is the scenario when RF and D are large. As result, we anticipate that the combination of effects coming from RF and D is responsible by the unfolding of the SG phase in two. To be precise, at

$T = 0$, we find two solutions for the SG order parameter instead of one, i. e., the usual one for small RF and D and a new one for large RF and D . The phases corresponding to each solution have genuine phase transitions between them. Furthermore, since we also analyse the AvHSG model with a presence of a ferromagnetic interaction, one might expect that the unfolding happens not only with SG phase, but also with mixed phase. As consequence, one can also expect a complicated scenario of reentrant transitions between paramagnetic, SG and mixed phases. At $T \neq 0$, the transitions between these several phases can be not only first order but also second. Thus, one can have the multiplication of multicritical points.

It should be remarked the role of RF or D when acting alone. For instance, it is well known that $D > 0$ tends to destroy any magnetic long range order by favoring states $S = 0$. In its turn, previous results on the Ising van Hemmen model with RF [16] show that the RF tends to suppress the SG phase. Therefore, it is quite clear that neither the RF nor the D acting alone can produce the unfolding of phase obtained in our work. Lastly, it is worth mentioning a recent work by Morais et al [17] using a random crystal field (instead of a RF) following a bimodal distribution with a p fraction of the spins without the influence of the crystal field and $p - 1$ fraction under the influence of D . Their results show that when p increases, the SG phase appears even for large D .

This paper is structured as follows. In Section II, we discuss the model and give details of the analytic calculations in the anisotropic van Hemmen model with RF in order to obtain the order parameters. Our numerical solutions for the order parameters are summarized in phase diagrams which are displayed in Section III. The conclusion is presented in Section IV.

2. Model

The model is given by the Hamiltonian

$$H = -\frac{J_0}{N} \sum_{(i,j)} S_i S_j - \sum_{(i,j)} J_{ij} S_i S_j - \sum_i h_i S_i + D \sum_{i=1}^N S_i^2, \quad (1)$$

where the spins can assume values $S = \pm 1, 0$. In the first term, J_0 represents the uniform ferromagnetic interaction while D is the anisotropic crystal field. The disordered interaction J_{ij} is given by

$$J_{ij} = \frac{J}{N} [\xi_i \eta_j + \xi_j \eta_i], \quad (2)$$

in which ξ_i and η_i are independents random variables following the bimodal distribution

$$P(x_i) = \frac{1}{2} [\delta(x_i - 1) + \delta(x_i + 1)]. \quad (3)$$

The random field h_i is also distributed according to the bimodal distribution:

$$P(h_i) = \frac{1}{2} \delta(h_i + h_0) + \frac{1}{2} \delta(h_i - h_0), \quad (4)$$

The partition function can be written as

$$Z_N = Tr \exp \left[\frac{\beta J_0}{N} \left(\left(\sum_i S_i \right)^2 - \sum_i S_i^2 \right) + \frac{\beta J}{N} \left\{ \left(\sum_i (\xi_i + \eta_i) S_i \right)^2 - \left(\sum_i \xi_i S_i \right)^2 - \left(\sum_i \eta_i S_i \right)^2 - 2 \sum_i \xi_i \eta_i S_i^2 \right\} + \beta h_i \sum_i S_i - \beta D \sum_{i=1}^N S_i^2 \right], \quad (5)$$

with $\beta = 1/T$ (T is the temperature). The quadratic terms in Eq. (5) can be linearized by the Gaussian identity $\exp(\lambda a^2) = \frac{1}{\sqrt{2\pi}} \int_{-\infty}^{\infty} \left(\frac{-x^2}{2} + a\sqrt{2\lambda}x \right) dx$, introducing the SG order parameters

$$q_1 = \frac{1}{N} \sum_i \langle\langle \xi_i S_i \rangle\rangle, \quad q_2 = \frac{1}{N} \sum_i \langle\langle \eta_i S_i \rangle\rangle. \quad (6)$$

and magnetization

$$m = \frac{1}{N} \sum_i \langle\langle S_i \rangle\rangle. \quad (7)$$

At the minimum free energy one has that $q_1 = q_2 = q$. Thereby, the free energy per spin is given as

$$\beta f = \frac{1}{2} \beta J_0 m^2 + \beta J q^2 - \langle\langle \ln [1 + 2e^{-\beta D} \cosh(\beta K)] \rangle\rangle, \quad (8)$$

with $K = J_0 m + J(\xi + \eta)q + h$. The equations for magnetization m and spin glass order parameter q follow from the saddle point equations: $\frac{\partial}{\partial m} \beta f = 0$ and $\frac{\partial}{\partial q} \beta f = 0$, respectively. Thus

$$m = \langle\langle \left\langle \frac{2e^{-\beta D} \sinh(\beta K)}{1 + 2e^{-\beta D} \cosh(\beta K)} \right\rangle \rangle \rangle \quad (9)$$

and

$$q = \frac{1}{2} \langle\langle \left\langle (\xi + \eta) \frac{2e^{-\beta D} \sinh(\beta K)}{1 + 2e^{-\beta D} \cosh(\beta K)} \right\rangle \rangle \rangle. \quad (10)$$

The symbol $\langle\langle \dots \rangle\rangle$ represents the averages on ξ , η and h which are performed using the distributions given in Eqs. (3)-(4).

It is also important to investigate the average magnetic occupation. Therefore, we also calculated $Q = \langle\langle S_i^2 \rangle\rangle$ which gives

$$Q = \langle\langle \left\langle \frac{2e^{-\beta D} \cosh(\beta K)}{1 + 2e^{-\beta D} \cosh(\beta K)} \right\rangle \rangle \rangle. \quad (11)$$

In the context of the present work, Q indicates not only whether the spin state on the sites are magnetically active to interact with other spins but also whether they are coupled with the RF.

3. Results

In this section, we present and discuss phase diagrams for: (i) $J_0 = 0$ which does give $m = 0$; (ii) $J_0 \neq 0$ which can give $m \neq 0$. Therefore, in general terms, one can distinguish four phases: (i) SG with $q \neq 0$ and $m = 0$; (ii) ferromagnetic with $q = 0$ and $m \neq 0$; (iii) paramagnetic with $q = 0$ and $m = 0$ and (iv) the mixed phase with $q \neq 0$ and $m \neq 0$. As we shall discuss below, these phases are unfolded into distinct thermodynamic phases with different numerical values for q , m and Q . We also remark that the crystal field D , h_0 and J_0 are given in units of J (see Eq. (2)).

3.1. Phase diagrams with $J_0 = 0$

3.1.1. Temperature $T = 0$

Firstly, it should be remarked that the RF prevents any induced magnetization. Therefore, for $J_0 = 0$, it is ruled out any finite induced or spontaneous magnetization.

We display in Fig (1) the possible ground states in the phase diagram D vs h_0 . In the Table I are shown the respective numerical values of q and Q . There are two regions to be considered initially, large h_0 and small D and vice-versa. In the first region, for large D/J and small h_0/J , it is found the NM phase while in the second one, for small D/J and large h_0/J , it is found the PM phase. The NM and PM phases have $Q = 0$ and 1, respectively. In the region NM, since $Q = 0$, most of the spin states in the sites are magnetically non-actives preventing, therefore, any spin glass ordering. In contrast, in the PM phase most of the spin states are magnetically active. However, there is no spin glass solution which indicates that for $Q = 1$, the RF also prevents any spin glass ordering. Thus, both situations have $q = 0$ but with distinct values for Q . The situation is utterly changed for small h_0/J and D/J ($D/J + h_0/J < 3/4$, $D/J < 1/2$ and $h_0/J < 1/2$). There, one can expect the existence of the usual spin glass ordering found in the AvHSG model (SG₁ in the Fig. (1) with $q = 1/2$) since there are conditions for the dominance of a spin glass ordering provided by the random interaction of the AvHSG model. Much less obvious is the existence of a second spin glass ordering (SG₂ in the Fig. (1) with $q = 1/4$). The mechanism for the onset of SG₂ phase is uncommon. For a certain combination of large h_0/J and D/J ($h_0/J - 1/4 < D/J < h_0/J + 1/4$ and $D/J + h_0/J > 3/4$), the dilution of magnetically active sites favored by D/J competes with the disordered site activation provided by the increase of h_0/J and creates again the dominance of a spin glass ordering. Therefore, the SG phase is unfolded in two distinct phases SG₁ and SG₂.

We remark another important difference between SG₁ and SG₂ phases as compared with NM and PM phases. For instance, in the NM and PM phases, the magnetic occupation Q does not depend on h_0 . In contrast, inside the SG₁ and SG₂ phases, the behavior of Q is determined by the relationship $D \leq h_0$ as can be seen in Table 1. As consequence, the dotted line in Fig. (1) represents a crossover line separating regions with distinct values of Q inside the same phase (SG₁ or SG₂) which reflects a fine balance which determines distinct amounts

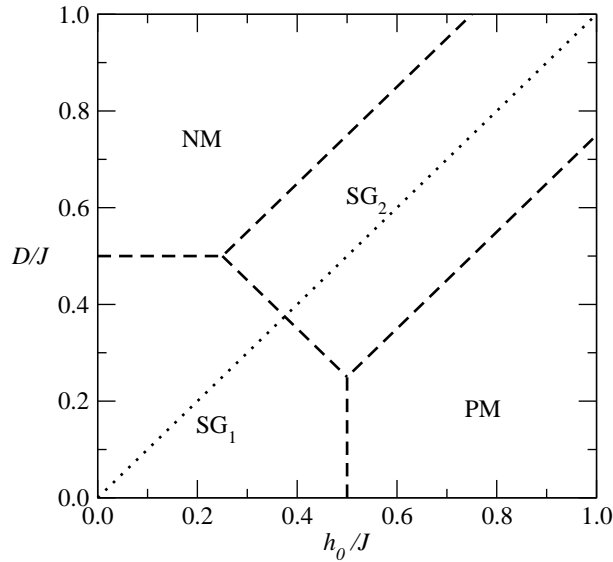


Figure 1: Phase diagram D/J vs h_0/J at $T = 0$ with $J_0 = 0$. The order parameters and the average magnetic occupation per site Q of each phase are given in Table 1. The dashed lines represent first order line transitions. The dotted line represents a crossover line separating the behavior of Q in the SG_1 and SG_2 phases for $D \lesseqgtr h_0$.

of magnetically active sites inside SG_1 and SG_2 phases above and below the line $D = h_0$. It should be mentioned that the boundaries lines of the four phases discussed above Fig. (1) are first order ones. As consequence, there are two triple points in the phase diagram.

Table 1: Phases, Order Parameters and $Q = \langle S_i^2 \rangle$

Phases	m	q	Q
PM	0	0	1
SG_1	0	1/2	1 ($D < h_0$)
SG_1	0	1/2	1/2 ($D > h_0$)
SG_2	0	1/4	3/4 ($D < h_0$)
SG_2	0	1/4	1/4 ($D > h_0$)
NM	0	0	0

3.1.2. Temperature $T \neq 0$

The effects of temperature increase the complexity of the problem bringing the presence of tricritical and ordered critical points. The sequence of phase diagrams displayed in the Figs. (2)-(4) has constant $D/J = 0.45, 0.49$ and 0.6 , respectively. We point out that the phase diagrams have topology similar with those ones found in Blume-Capel model with a RF given in Ref. [19].

The values of D/J chosen above select three distinct types which can be organized in terms of the presence of tricritical and ordered critical points. It is well known that, at mean field level, one can find in a 3-state spins models the presence of tricritical points which can have two sources: (i) due to the favoring of $S = 0$ states at lower temperature as D increases (for instance, a the Blume-Capel model [18]) and ; (ii) reminiscent of Ising limit ($D \rightarrow -\infty$) of the AvHSG model with bimodal RF. We named the tricritical points related with the scenario discussed in (i) and (ii) as TC_1 and TC_2 , respectively.

The first type of phase diagram can be seen in Fig. (2). At lower temperature, SG_1 and SG_2 phases are separated by a first order line transition ending at an ordered critical point. Then, SG_1 and SG_2 phases become identical. Consequently, there is a second order phase line transition separating the PM phase from the spin glass phase. This second order line becomes a first order one at the TC_2 point. The second type of phase diagram is displayed in Fig. (3). Besides the presence of an ordered critical point and the TC_2 point, there is also the emergence of the TC_1 point for smaller h_0/J . Other interesting aspect is that the paramagnetic phase is splitted into NM and PM phases. The presence of NM phase for smaller h_0/J suggests that the TC_1 point can be related with the phase transition between the NM (instead of PM) and any spin glass phase. This relationship is well illustrated in Fig. (4). In the phase diagram shown in that figure, the only remaining ordered phase is SG_2 existing in a dome-shaped region. Thus, there is no longer an ordered critical point. The phase transition line between the SG_2 phase and NM for smaller h_0/J and, then, PM phases for larger h_0/J present TC_1 and TC_2 points. Their location were also checked by the expansion of free energy in terms of the SG order parameter in the Appendix.

3.2. Phase diagrams with $J_0 \neq 0$

3.2.1. Temperature $T = 0$

The presence of ferromagnetic interaction $J_0 \neq 0$ brings the possibility of finite spontaneous magnetization and, as consequence, the arising of mixed or ferromagnetic phases. In order to find such phases, we choose $J_0/J = 1/2$ and 1.

In the case $J_0/J = 1/2$, Table II provides the numerical values for the m , q and Q corresponding to each phase in Fig. (5). The phases SG_1 , SG_2 , NM and PM have the same numerical values for these quantities already displayed in Table I. In addition, there is the emergence of mixed phases. It is well established the existence of a mixed phase in the AvHSG model without a RF. Nevertheless, our results show that not only part of the spin glass phase, which is already unfolded, is replaced by a mixed one but also the mixed phase is unfolded in four distinct phases (M_1 , M_2 , M_3 and M_4 in Fig. (5)) with first order transition separating them and the SG_1 and SG_2 phases. Each one, M_1 , M_2 , M_3 or M_4 have a different combination of numerical values for q , m and Q (see Table II). For instance, inside of the SG_1 phase there is the emergence of the M_1 phase for very small values of D/J and h_0/J ($D/J + h_0/J < 7/40$,

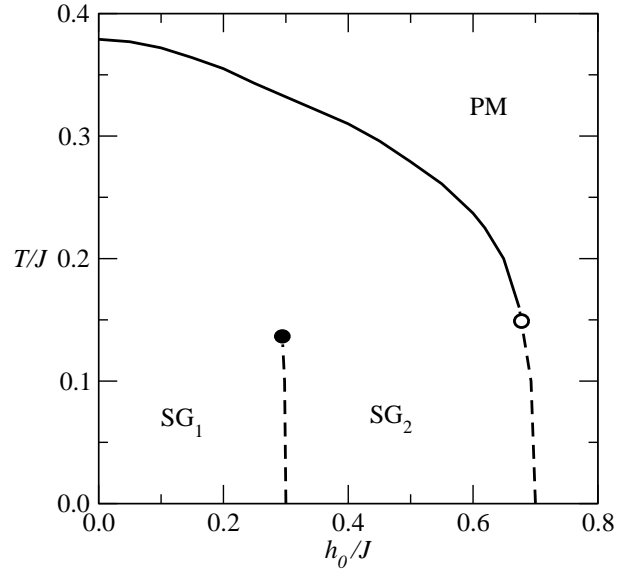


Figure 2: Phase diagram T/J vs h_0/J for $D = 0.45J$ presenting one ordered critical point (filled circle) and one tricritical point (open circle). The dashed lines represent first order line transitions.

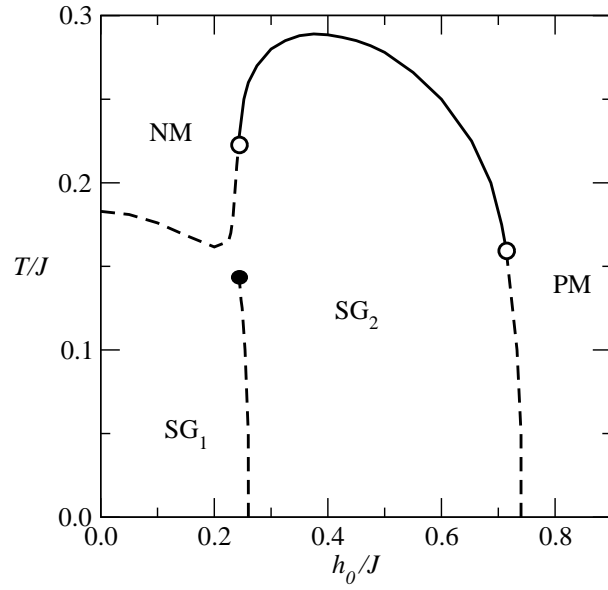


Figure 3: Phase diagram T/J vs h_0/J for $D = 0.49J$ presenting one ordered critical point (filled circle) and two tricritical points (open circles). The dashed lines represent first order line transitions.

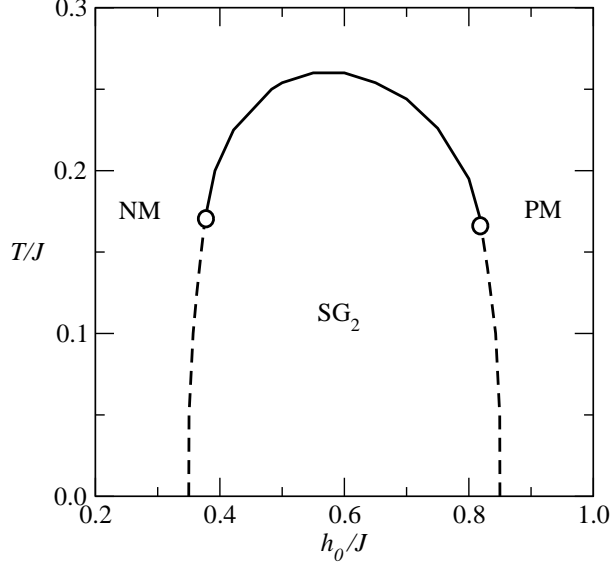


Figure 4: Phase diagram T/J vs h_0/J for $D = 0.6J$ presenting two tricritical points (open circles). The dashed lines represent first order line transitions.

$D/J < 5/40$ and $h_0 < 5/40$) which corresponds to the usual mixed phase of the AvHSG model ($m = 1/2$, $q = 1/2$ and $Q = 1$). However, the emergence of M_2 , M_3 and M_4 is again not obvious. For these mixed phases, there is a fine balance of mechanisms driven by the energy scales h_0 , D and J_0 (given in units of J) within the region where the phases SG_1 and SG_2 are initially located. Then, inside the SG_1 phase appears also the M_2 phase ($7/40 < D/J + h_0/J < 18/25$ and $-3/40 < D/J - h_0/J < 3/40$). Inside the SG_2 appears the M_3 phase ($D/J + h_0/J > 18/25$ and $-3/40 < D/J - h_0/J < 3/40$). The M_4 phase appears between M_2 and M_3 phases ($18/25 < D/J + h_0/J < 39/50$ and $-3/40 < D/J - h_0/J < 3/40$). It should be also stressed that this fine balance affects also the average magnetic occupation per site with the sequence of jumps as can be seen in Table 2 from M_1 to M_4 . It should be mentioned that due to the number of phases with first order transitions between them, one has 8 triple points in Fig. (5). Another aspect to be mentioned is that for some fixed values of D , by varying h_0 (or vice-versa), the SG_1 and SG_2 phases are reentrant.

In the case $J_0/J = 1$ there is no longer spin glass or mixed phases which are entirely replaced by a ferromagnetic one. This phase is also unfolded depending on D/J and h_0/J . The corresponding FE_1 and FE_2 phases have m and Q given in Table III. That case recovers entirely the results obtained for the Blume-Capel model with RF given in Ref. [19].

3.2.2. Temperature $T \neq 0$

In this section we discuss only the case $J_0/J = 0.5$, since the case $J_0/J = 1$ reproduces exactly the results obtained in Ref. [19] at finite temperature.

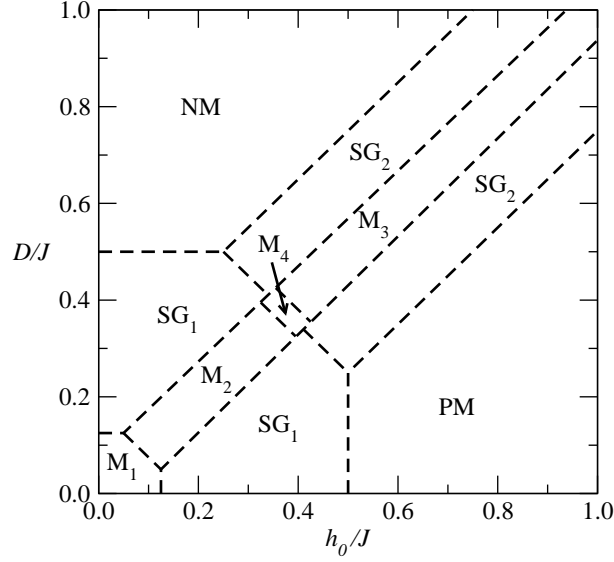


Figure 5: Phase diagram D/J vs h_0/J at $T = 0$ with $J_0/J = 0.5$. The order parameters and the average magnetic occupation per site Q of each phase are given in Table II. The dashed lines represent first order line transitions.

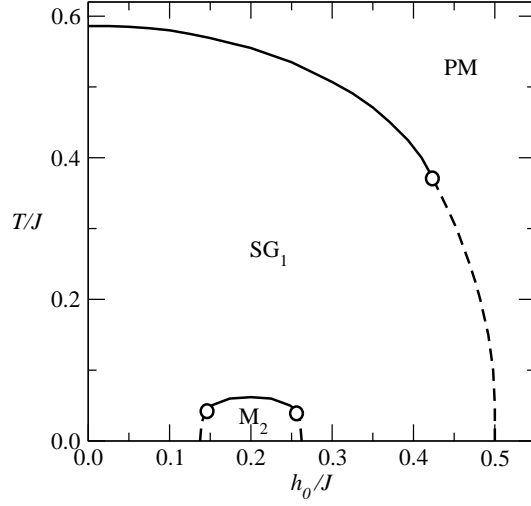


Figure 6: Phase diagram T/J vs h_0/J for $D = 0.2J$ presenting three tricritical points (open circles). The dashed lines represent first order line transitions.

Table 2: Phases, Order Parameters and $Q = \langle S_i^2 \rangle$

Phases	m	q	Q
PM	0	0	1
M ₁	1/2	1/2	1
M ₂	1/4	1/2	3/4
M ₃	1/4	1/4	1/2
M ₄	3/8	3/8	5/8
SG ₁	0	1/2	1 ($D < h_0$)
SG ₁	0	1/2	1/2 ($D > h_0$)
SG ₂	0	1/4	3/4 ($D < h_0$)
SG ₂	0	1/4	1/4 ($D > h_0$)
NM	0	0	0

Table 3: Phases, Order Parameters and $Q = \langle S_i^2 \rangle$

Phases	m	q	Q
FE ₁	1	0	1
FE ₂	1/2	0	1/2
NM	0	0	0
PM	0	0	1

In Figs (6)-(11) are shown phase diagrams T/J vs h_0/J with $D/J = 0.2, 0.3, 0.375, 0.403, 0.45$ and 0.6 , respectively. These choices for values of D allow to display the most interesting types of phase diagrams in terms of multicritical points. These phase diagrams are even more complex as those ones displayed in Section 3.2.1 since the number and the variety of multicritical points are enhanced.

As a whole, the features observed in Fig. 6 are preserved in Figs. (7 - 11), but there are additional features that deserve discussion. These figures are representative examples of T/J vs. h_0/J phase diagrams that are observed in the interval $1/4 < D/J < 1/2$, where phases SG₁ and SG₂ coexist at low temperature. The first-order line between them ends in a critical point. It moves in the diagram from the right, like in Fig. (7), to the left, like in Fig. (10), as D/J increases. Figure (7) corresponds to $D = 0.3$. The dome shaped region is a M₂ phase, at the left of the first-order line. Figure (10) corresponds to $D = 0.45$. The dome shaped region is a M₃ phase, at the right of the first-order line. Figures (8) and (9), for $D/J = 0.375$ and $D/J = 0.403$, respectively, show the interesting situation where the first-order line goes through the dome shaped region, giving rise to the appearance of the M₄ subphase. In Fig. (8) M₄ appears between M₂ and M₃. Consequently, this figure shows a triple point intersecting two second-order lines. The triple point joins first-order lines that separate phases with three distinct q , values. These are: $q = 0.5$ in phases

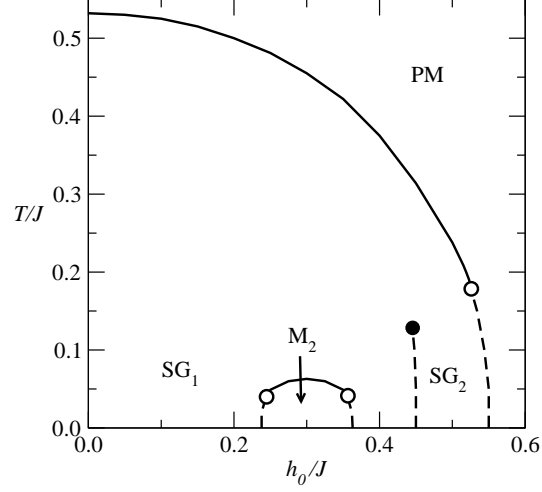


Figure 7: Phase diagram T/J vs h_0/J for $D = 0.3J$ presenting one ordered critical point (filled circle) and three tricritical points (open circles). The dashed lines represent first order line transitions.

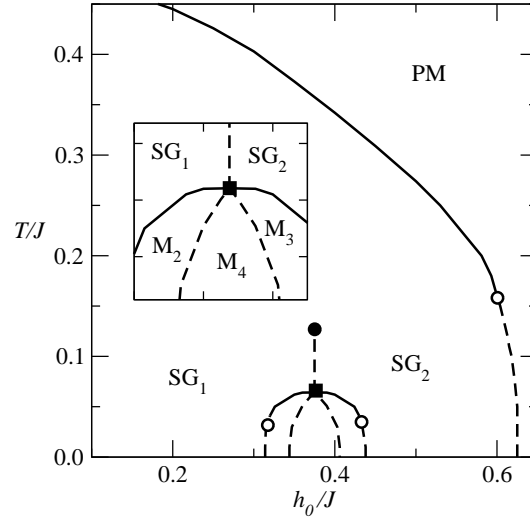


Figure 8: Phase diagram T/J vs h_0/J for $D = 0.375J$ presenting one ordered critical point (filled circle), one triple point over a second order line (filled square) and three tricritical points (open circles). The dashed lines represent first order line transitions. For a better visualization, the inset shows a “zoom” of the region with the triple point over the second-order line.

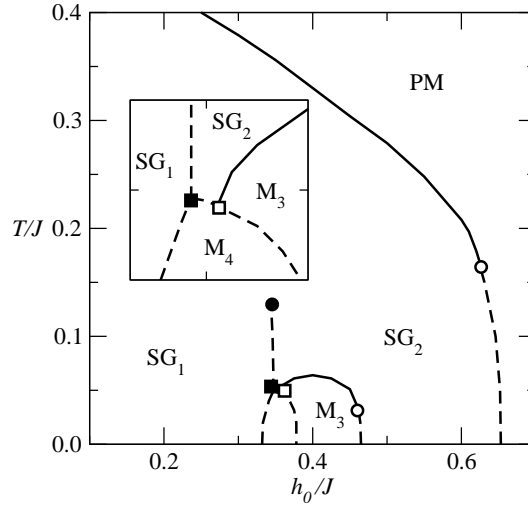


Figure 9: Phase diagram T/J vs h_0/J for $D = 0.403J$ presenting one ordered critical point (filled circle), one triple point (filled square), one critical endpoint (open square) and two tricritical points (open circles). The dashed lines represent first order line transitions. For a better visualization, the inset shows a “zoom” of the region with the triple point and the critical endpoint.

M_2 and SG_1 ; $q = 0.375$ in phase M_4 ; $q = 0.25$ in phases M_3 and SG_2 . The second order line separates the continuous transition from $m > 0$, in phases M_2 and M_3 to $m = 0$, in phases SG_1 and SG_2 . In Fig. (9) M_2 is absent, and the phase diagram shows a triple point between SG_1 , SG_2 and M_4 and a critical endpoint where M_4 makes first-order transitions with SG_2 and M_3 and M_3 makes a second-order transition to SG_2 .

In Fig. (11), the situation is completely changed. According to Fig. (5), there SG_1 phase is no longer present at $T/J = 0$ if $D/J > 1.2$ and, consequently it should not be found at finite T . There is only the SG_2 phase which occupies a dome-shaped spin glass region. Similarly to the phase diagram shown in Fig. (4), the paramagnetic phase is splitted in NM (smaller h_0/J) and PM (larger h_0/J) ones. Consequently, one has again TC_1 and TC_2 points. Furthermore, at lower temperature there is a reentrant M_3 phase occupying a dome-shaped region inside the SG_2 phase. In the transition line between SG_2 phase to M_3 one also has two tricritical points.

4. Conclusions

We studied the 3-state van Hemmen spin glass model in the presence of a bimodal RF, in a mean-field approximation, in three different scenarios: i) in the absence of uniform ferromagnetic interaction ($J_0 = 0$), where only spin glass, paramagnetic and non-magnetic phases are present; ii) in the presence of a moderate uniform ferromagnetic interaction ($J_0/J = 1/2$) where, in addition to

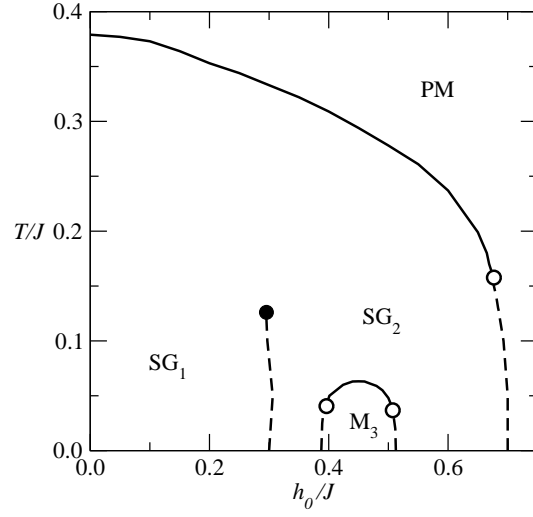


Figure 10: Phase diagram T/J vs h_0/J for $D = 0.45J$ presenting one ordered critical point (filled circle) and three tricritical points (open circles). The dashed lines represent first order line transitions.

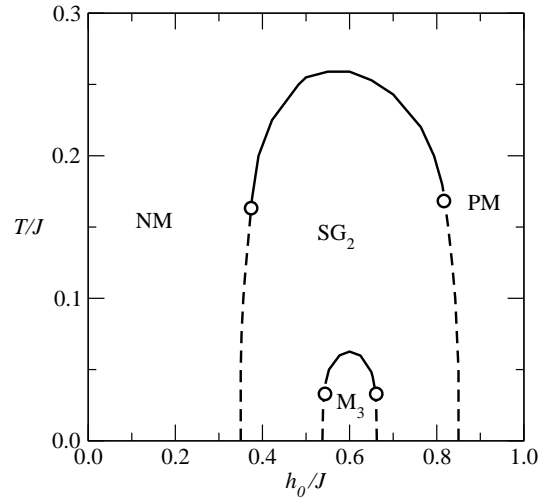


Figure 11: Phase diagram T/J vs h_0/J for $D = 0.6J$ presenting four tricritical points (open circles). The dashed lines represent first order line transitions.

the phases mentioned above, mixed phases were observed; iii) in the presence of a strong uniform ferromagnetic interaction ($J_0/J = 1$), we found ferromagnetic phases, besides the paramagnetic and non-magnetic phases. For this particular case, the phase diagrams reproduce the results found for the Blume-Capel model with a random field given in Ref. [19]. It is worth to remember that non-magnetic and paramagnetic phases differ only in the occupation per site Q .

For $J_0 = 0$, the zero-temperature D/J vs. h_0/J phase diagram displays the unfolding of SG phase in two distinct phases labeled SG_1 and SG_2 . Such unfolding appears as a fine balance between the RF (that favors active states $S_i = \pm 1$) and the crystal field D (that favors $S_i = 0$). Furthermore, in both SG_1 and SG_2 the occupation per site changes discontinuously over the diagonal $D/J = h_0/J$ at $T/J = 0$. For finite temperature, besides one or two (for the dome shaped SG region) tricritical points, there is also the emergence of a critical point related to the unfolding of the SG phase.

Far more interesting is the situation for $J_0 = 1/2$, with the appearing of several mixed phases and an unusual scenario of triple points and multicritical points. The zero temperature D/J vs. h_0/J phase diagram shows four mixed phases, labeled M_1 to M_4 , located near the diagonal $D/J = h_0/J$, inside the two spin glass phases. By fixing D/J we obtain several T/J vs. h_0/J phase diagrams, where the mixed phases appear as a dome shaped region inside a spin glass phase. The most intriguing ones are those where the mixed phase dome interacts with the first-order line between SG_1 and SG_2 , at low temperature, giving rise or to a triple point intersecting two critical lines or a triple point close to a critical endpoint.

Next, we briefly discuss the contribution of our work as compared with previous studies of magnetic models with RF. In fact, the results obtained in the Blume-Capel model [19] or in the Ising van Hemmen model [16] both with RF can be considered limit situations of our model. The first case corresponds to the situation where $J_0 \gg J$ while the second one corresponds to $D \rightarrow -\infty$. Moreover, the AvHSG model with uniform field [15] is also contained in our model if the RF distribution in Eq. 4 is generalized as $P(h_i) = (1 - p)\delta(h_i + h_0) + p\delta(h_i - h_0)$ taking the limit $p \rightarrow 1$.

We emphasize that the most important result of our work is to show how the combined effects of D and RF can create conditions to stabilize SG and mixed phases. That is far from obvious, since the effects of D and RF taken individually tends to suppress these phases (at least, at mean field level). Particularly, this result leads to a complicate scenario of reentrant phases when the RF increases. Surely, there is a subtil mechanism. At $T = 0$, for small D and RF, it is quite clear that the random interaction is the dominant energy scale. Nevertheless, when RF and D increase, they do compete, but mainly to establish an average magnetic occupation which is neither $Q = 1$ (spins totally active) nor $Q = 0$ (spins totally non-active). The main consequence is that there are still spins available ($0 < Q < 1$) to interact via random interaction and, eventually, via ferromagnetic interaction as well. That is the reason because SG and the mixed phases stabilise but with order parameter smaller than the corresponding values with small RF and D . We believe that this mechanism is independent of any

specific choice of random field distribution. It should be remarked that there is one common aspect of our result with those ones found in the Ref. [19]. That is the unfolding of phases as well as the proliferation of multicritical points. As demonstrated in our work, we can recover entirely the results of Ref. [19] when the ferromagnetic interaction overcomes the random one. Indeed, what we are demonstrating is how those results can develop as long as disordered interaction is being added.

Although our results refer a particular model, we expect that our results can shed light in problems containing the interplay among random interaction and field, ferromagnetic interaction and crystal field. A possible physical realization of such scenario might be found, for instance, in martensitic alloys. In these systems, it has been established the existence of strain glasses which is the analogue of SG concerning lattice distortions. In this glassy phase, there are local random configurations of lattice distortion [22, 23]. Finally, we would like to remark that our study does not aim to be exhaustive. So, it is not excluded the possibility for more complicated features, in terms of multicritical points, for different values of D or J_0 . On other hand, we remark that we are doing a mean field theory. The existence of some multicritical points may be related with this level of description (see, for instance, [20, 21]).

Acknowledgments

The present study was supported by the brazilian agencies Conselho Nacional de Desenvolvimento Científico e Tecnológico (CNPq) and CAPES. The authors acknowledge Profs. M. C. Barbosa and J. J. Arenzon for useful discussions.

5. Appendix

The tricritical points TC_1 and TC_2 are obtained from the expansion of the free energy (see Eq. (8)). Therefore:

$$f - f_0 = \frac{Ja_2}{K_0^2}q^2 + \frac{2\beta^3 J^4 a_4}{3K_0^4}q^4 + \frac{4\beta^5 J^6 a_6}{45K_0^6}q^6 \quad (12)$$

where $\beta f_0 = -\ln[1 + 2e^{-\beta D} \cosh(\beta h_0)]$ and

$$a_2 = e^{2\beta D} + (2 - \beta J)2e^{\beta D}w + (1 - \beta J)4w^2 + 4\beta Jv^2, \quad (13)$$

$$a_4 = e^{3\beta D}w - 12e^{\beta D}w^3 - 16w^4 - 8e^{\beta D}(e^{\beta D}v^2 - 2wv^2) + 64w^2v^2 - 48v^4 \quad (14)$$

$$a_6 = -e^{5\beta D}w + 20e^{4\beta D}w^2 + 80(e^{3\beta D}w^3 - e^{2\beta D}w^4) - 560e^{\beta D}w^5 - 512w^6 + 32e^{4\beta D}v^2 - 344e^{3\beta D}wv^2 - 676e^{2\beta D}w^2v^2 + 2464e^{\beta D}w^3v^2 + 4352w^4v^2 - 960e^{2\beta D}v^4 - 1920e^{\beta D}wv^4 - 7680w^2v^4 + 3840v^6 \quad (15)$$

with $w = \cosh(\beta h_0)$, $v = \sinh(\beta h_0)$ and $K_0 = e^{\beta D} + 2 \cosh(\beta h_0)$. To obtain the second order line transition, we use $a_2 = 0$ and $a_4 > 0$. The tricritical points are located when $a_2 = 0$, $a_4 = 0$ and $a_6 > 0$.

References

- [1] D. P. Belanger, in *Spin Glasses and Random Fields*, edited by A. P. Young (World Scientific, Singapore, 1998), p. 251.
- [2] M. Gingras, P. Henelius, J. Phys: Conf. Ser. **320**, 012001 (2011).
- [3] R. F. Soares, F. D. Nobre and J. R. L. de Almeida, Phys. Rev. B **50**, 6151 (1994)
- [4] G. Parisi, J. Phys. A **13**, 1101 (1980); *ibid.* 1887 (1980).
- [5] J. R. L. de Almeida, D. J. Thouless, J. Phys. A **11**, 983 (1978).
- [6] J. A. Mydosh, Rep. Prog. Phys. **78**, 052501 (2015).
- [7] S.K. Ghatak and D. Sherrington, J. Phys. C **10**, 3149 (1977).
- [8] F. A. da Costa, C. S. O. Yokoi, S. R. Salinas, J. Phys. A **27**, 3365 (1994).
- [9] C. V. Morais, M. J. Lazo, F. M. Zimmer, S. G. Magalhaes, Phys. Rev. E **85**, 031133 (2012)
- [10] C. V. Morais, M. J. Lazo, F. M. Zimmer, S. G. Magalhaes, Physica A **392**, 1770 (2013)
- [11] C. V. Morais, F. M. Zimmer, M. J. Lazo, S. G. Magalhaes, F. D. Nobre, Phys. Rev. B **93**, 224206 (2016).
- [12] J. L. van Hemmen, Phys. Rev. Lett. **49**, 409 (1982).
- [13] J. L. van Hemmen, A.C.D. van Enter, J. Canisius, Z. Phys. B - Condensed Matter **50**, 311 (1983).
- [14] T. C. Choy, D. Sherrington, J. Phys. C: Solid State Phys. **17**, 739 (1984).
- [15] J. R. L. de Almeida, F. C. Brady Moreira, Z. Phys. B - Condensed Matter **63**, 365 (1986).
- [16] Y. Nogueira, J. R. Viana, J. R. de Souza, Braz. J. Phys. **37** 331 (2007)
- [17] D. N. de Morais, M. Godoy, A. S. de Arruda J. N. da Silva, J. R. de Souza, J. Magn. Magn. Mater. **398** 253-258 (2016)
- [18] M. Blume, Phys. Rev., **141**, 517 (1966). H.W. Capel, Physica, **32**, 966 (1966).
- [19] M. Kaufman, M. Kanner, Phys. Rev. B **42**, 2378 (1990).

- [20] R. Erichsen Jr., A. A. Lopes, S. G. Magalhaes, Phys. Rev. E **95**, 062113 (2017).
- [21] F. Doria, R. Erichsen Jr., D. Dominguez, M. Gonzalez, S. G. Magalhaes, Physica A **422**, 58 (2016).
- [22] D. Sherrington, Phys. Status Solidi, **251**, 1967 (20014).
- [23] R. Vasseur, T. Lookman, Phys. Rev. B, **81**, 094107 (2010).